High-Temperature Symmetry Breaking in the Electronic Band Structure of the Quasi-One-Dimensional Solid $NbSe_3$

J. Schäfer,[1,2] Eli Rotenberg,[1] S. D. Kevan,[3] P. Blaha,[4] R. Claessen,[2] and R. E. Thorne[5]

[1]*Advanced Light Source, Lawrence Berkeley National Laboratory, Berkeley, California 94720*
[2]*Institut für Experimentalphysik, Universität Augsburg, 86135 Augsburg, Germany*
[3]*Department of Physics, University of Oregon, Eugene, Oregon 97403*
[4]*Institut für Physikalische und Theoretische Chemie, Technische Universität Wien, 1060 Wien, Austria*
[5]*Laboratory of Atomic and Solid State Physics, Cornell University, Ithaca, New York 14853*

(Received 14 February 2001; published 23 October 2001)

The electronic band structure of the Peierls compound $NbSe_3$ has been explored for its symmetries with microspot synchrotron photoemission. The Fermi level crossings and deviations from one-dimensional behavior are identified. Density-functional calculations of the Fermi surfaces confirm the nesting conditions relevant for the two phase transitions. The instability along the chains with superstructure periodicity $q = 0.44$ Å^{-1} induces a backfolding of the electronic bands, and the Fermi level crossings appear suppressed. This broken symmetry is observed in the fluctuation regime at more than twice the critical temperature, where the correlation length is strongly reduced.

DOI: 10.1103/PhysRevLett.87.196403 PACS numbers: 71.30.+h, 71.18.+y, 71.20.Lp, 79.60.Bm

One-dimensional (1D) solids are of great interest because of the many unusual phenomena they may exhibit, such as Peierls instabilities [1] and deviations from Fermi liquid behavior [2]. Photoemission appears particularly suited to probe these exotic electronic properties [3]. An important topic is the effect of Peierls instabilities on the periodicity of experimentally determined electron bands. In the simplest case of a half-filled band, a Peierls distortion leads to a new Brillouin zone of half the original width. More generally, a charge density wave (CDW) can induce a zone that is incommensurate with the underlying lattice. It lifts the original symmetry of the lattice and leads to a total loss of translational symmetry. Electronic band structure, often derived from translational invariance, can still exist in systems with incommensurate periodic potentials [4]. Yet the regime above the phase transition, where CDW precursor fluctuations are present, has not sufficiently been explored. One of the most intriguing compounds in this respect is $NbSe_3$ with its two incommensurate charge density waves.

$NbSe_3$ crystals take the form of needlelike whiskers roughly 10 μm in diameter that are easily cleaved into fine fibers. Its structural properties thus already point at pronounced 1D character. $NbSe_3$ exhibits CDW transitions at $T_1 = 145$ K and $T_2 = 59$ K, which both lead to a significantly reduced Fermi surface as seen in resistivity measurements [5]. Only the T_1 CDW is directed along the main axis. This transition induces a low temperature energy gap of $2\Delta = 170$ meV, detected by tunneling spectroscopy [6,7]. The mean field transition temperature calculated from this value is $T_{MF} \sim 580$ K. For such a system, thermal fluctuations suppress a charge ordered state, and for an ideal 1D system no phase transition should be observable at low temperature. Typical discrepancies between T_{MF} and the observed transition temperature are of the order of a factor of 2 or more [8]. The ratio amounts to 3.1 for $(TaSe_4)_2I$. For $NbSe_3$ the dramatic discrepancy of $T_{MF} : T_1 \sim 4.0$ makes it immediately apparent how well some states are confined to 1D. The compound hence is the primordial system for the study of CDW phenomena. A key question still open is on the nesting conditions in the electron bands.

In this Letter, we address the interplay of local symmetries and electronic band structure in $NbSe_3$ in the presence of fluctuations. Owing to the difficulty to prepare the minute samples, photoemission data have not previously been available. Using a microfocused synchrotron beam, angle-resolved photoemission is now successfully achieved for the first time and serves to determine the bands that supply the nesting conditions for the CDW wave vectors. This is complemented by a modern density functional theory (DFT) calculation of the Fermi surfaces. Data taken far above the CDW phase transition temperature T_1 reveal a persistent supercell zone boundary with strict band structure backfolding not previously observed in this regime.

High-purity samples were grown as previously described [9]. The $NbSe_3$ whiskers were suspended freely on a sample holder and then cleaved in vacuum. This exposes the b-c plane of the surface, as referred to below. Photoemission was performed at beam line 7.0.1 at the Advanced Light Source in Berkeley. The incident light beam was focused to a spot size of approximately 50 μm to ensure that only the whiskers were illuminated. With a Phi brand hemispherical analyzer, energy resolution amounted to ~50 meV, angular resolution to $\sim\frac{1}{2}°$. All measurements were performed at $T = 300$ K.

An overview of the experimental band structure along the strands, obtained at $h\nu = 100$ eV, is given in Fig. 1. For the crystal lattice of $NbSe_3$ with its monoclinic unit cell [10] we adopt the following Brillouin zone dimensions [11]: depth $a^* = 0.6658$ Å^{-1}, length in chain

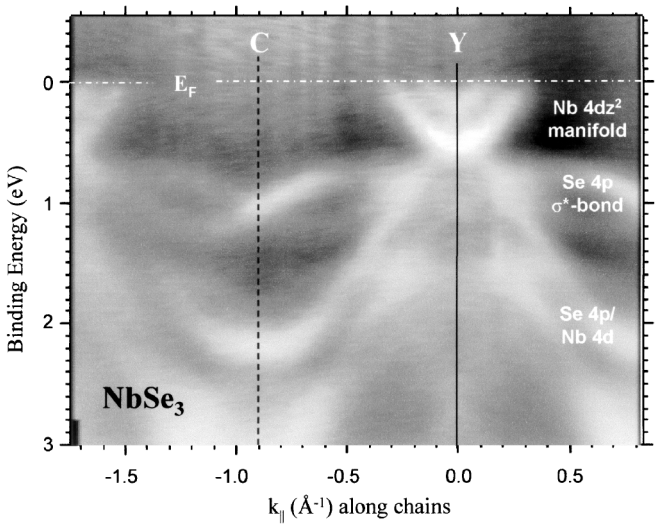

FIG. 1. Electronic band structure along the whiskers (b^* axis, data normalized to angle-integrated spectrum). Near the Fermi level two sets of parabolic bands are clearly discernible. They originate from Nb $4d$ states and supply the nesting conditions for the CDWs.

direction $b^* = 1.8055$ Å^{-1}, and width $c^* = 0.4264$ Å^{-1} (forming an angle of 70.53° with a^*). The perpendicular momentum (at $h\nu = 100$ eV and assuming an inner potential of 10 eV) is roughly estimated as $k_\perp \approx (7\frac{1}{2})a^* = Y$, the zone boundary in the depth of the Brillouin zone. The features of the band map relevant for our study are the two sets of parabolic bands that cross the Fermi level.

Electronic bands were calculated in the tight-binding method by Canadell *et al.* [12] and Shima [13]. The latter author determined partial densities of states, assigning the bands around 1 eV to Se $4p$ σ^* bonds, below which are Se $4p$ states partially hybridized with Nb $4d$. The topmost bands are of Nb d_{z^2}-type, as indicated in Fig. 1. Crystal field splitting and nonzero interchain interaction lifts the degeneracy of the levels at the Fermi energy E_F. This splitting is responsible for the CDW nesting conditions. Canadell *et al.* predict four bands to cross E_F, whereas Shima claims a fifth band. Those closely adjacent bands are not seen individually in the data. The DFT analysis of the present work resolves this issue and produces five bands with states at E_F.

Fermi surfaces and band structure of $NbSe_3$ have been calculated using the DFT method within the generalized gradient approximation [14] and a relativistic self-consistent full-potential linearized augmented plane wave procedure [15]. Fermi surface cross sections for principal directions are computed as constant energy surfaces. The result for the a^*-b^* plane vertically cut into the sample along the chain direction is shown in Fig. 2a. We obtain five Fermi surfaces (FS) which all have a weak curvature in this cross section. The five Fermi level crossings on the Γ-Z line are at 0.08 Å^{-1}, 0.10 Å^{-1}, 0.22 Å^{-1} (double crossing) and at 0.30 Å^{-1}.

The nesting vectors in units of (a^*, b^*, c^*) determined from diffraction measurements are $\mathbf{q}_1 = (0, 0.241, 0)$ for the $T_1 = 145$ K CDW and $\mathbf{q}_2 = (0.5, 0.259, 0.5)$ for the $T_2 = 59$ K CDW [7,10], and are both incommensurate. The calculated Fermi contours that provide a nesting condition are outlined in Figs. 2b and 2c. Within a single FS, no matching condition is found. Instead, pairs of FS supply the nested areas: pair 2–3 for $\mathbf{q}_1$ and pair 1–4 for $\mathbf{q}_2$, as indicated in the diagram. The mechanism as such was first suggested by Shima [13], although the accuracy of his calculation could not deliver a solution for $\mathbf{q}_2$. The need to refer to a Coulomb interchain interaction to account for the discrepancy becomes obsolete in the DFT result, although such interaction may still exist. Both Peierls distortions introduce a superstructure with new zone boundaries (ZB), which are obtained from geometric calculation and marked in Fig. 2. The length of $\mathbf{q}_1$ and hence the zone width for the distortion along the chains is $\mathbf{q}_1 = 0.44$ Å^{-1}. For $\mathbf{q}_2$, two mirror-symmetric, diagonal nestings are valid; therefore one obtains four diagonal zone boundaries.

The photoemission angle scan along the chain direction through Γ in Fig. 3 shows two bands approaching the Fermi level. The lower, approximately parabolic band (band 1) with a minimum at ~0.58 eV is the deepest one predicted by the DFT calculation, while the upper band with a minimum at ~0.28 eV is doubly degenerate (bands 2 and 3). This degeneracy is reflected in the Fermi surfaces of Fig. 2. The calculation predicts bands 4 and 5 to have shallow minima at 0.20 and 0.10 eV, respectively. They are not distinguishable experimentally (probably due

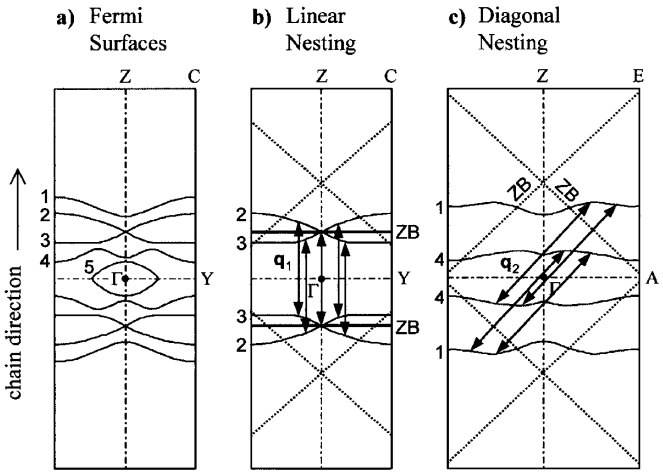

FIG. 2. Fermi surfaces (FS) of $NbSe_3$ calculated with DFT. (a) The total of five FS is seen in a cross section along chain direction and $k_\perp$. (b) Nesting of $\mathbf{q}_1$ along the chains, connecting FS 2 and 3. (c) Nesting of $\mathbf{q}_2$ in diagonal plane, connecting FS 1 and 4 (mirror-symmetric solution for $\mathbf{q}_2$ also valid). Zone boundaries (ZB) resulting from $\mathbf{q}_1$ and $\mathbf{q}_2$ are outlined with solid and dashed lines, respectively.

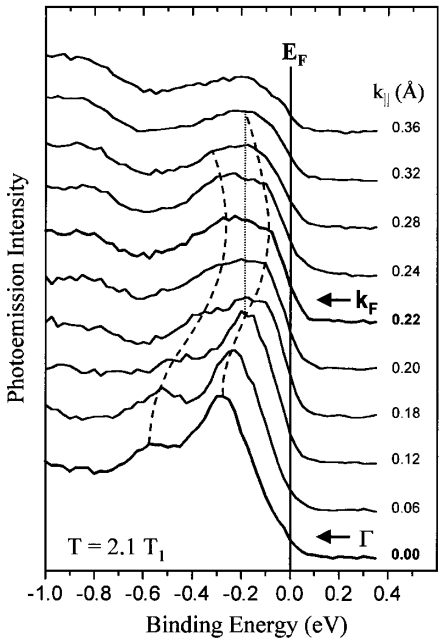

FIG. 3. Photoemission spectra at $T = 300$ K along Γ-Z where $\mathbf{q}_1$ is nested ($h\nu = 70$ eV, raw spectra). At $k_F = 0.22$ Å^{-1}, the leading edge is closest to E_F. For $k_\parallel > k_F$ backfolded intensity is observed, with peak positions symmetric around k_F. Dashed lines are a guide to the eye.

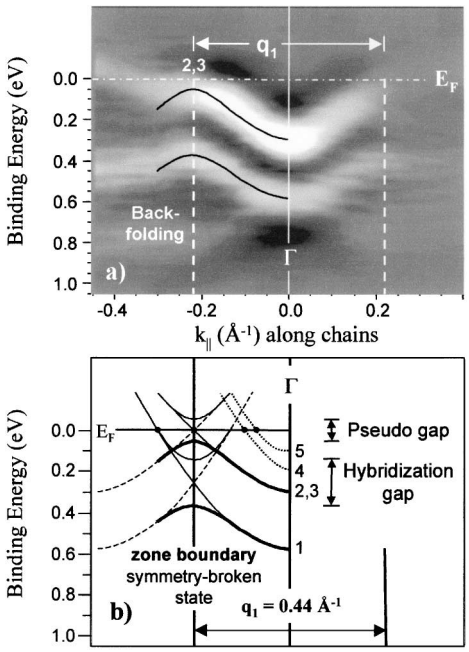

FIG. 4. Band structure symmetry lines. (a) Band map of the same region as in Fig. 3 (data normalized to angle-integrated spectrum and displayed as $-d^2I/dE^2$). (b) Band diagram using DFT Fermi level crossings. Backfolding at the $\mathbf{q}_1$ zone boundary is superimposed by the CDW precursor fluctuations.

to low cross section and finite resolution) yet are not nested in chain direction and leave the analysis unaffected.

The upper band (degenerate bands 2 and 3) exhibits a close approach to the Fermi level at $k_F = 0.22$ Å^{-1} which is excellently consistent with the DFT result. This immediately provides the nesting condition for $\mathbf{q}_1$. This to our knowledge is the first determination of the nesting condition for the CDW along the principal axis in $NbSe_3$. Although close to E_F, the band does not exhibit a metallic crossing. Instead, a loss of spectral weight is observed. Both upper and lower bands turn over at the same nested k value and then show incipient downward dispersion. Peak positions—not spectral weight—are approximately symmetric around k_F (compare, e.g., pairs of spectra at $k_F \pm 0.02$ Å^{-1}, or at $k_F \pm 0.10$ Å^{-1}).

The increasing loss of intensity for increasing $k > k_F$ is a characteristic of backfolded bands. The superstructure potential is usually weak compared to the potential of the unperturbed lattice [4]. Those bands are therefore also referred to as "shadow bands." Such fading intensity for a backfolded band has, e.g., been demonstrated for the spin density wave in chromium [16]. Further evidence for backfolding is the missing Fermi level crossing for the lower band. An approach of a peak to the Fermi level beyond k_F near 0.30 Å^{-1} (DFT) is not observed.

The backfolding occurs at a boundary which relates to the CDW zone of width $q_1 = 0.44$ Å^{-1}. Yet the data are recorded at room temperature which is $2.1 \times T_1$ and therefore far above the critical temperature. This observation would not be possible without precursor fluctuations of the Peierls state. Connection to the metallic phase can be made using the band map display of Fig. 4a. For better contrast, the data were normalized to the average of all spectra and then plotted as negative second derivative with respect to energy, $-d^2I/dE^2$. Although weak features at large k values may be affected by the normalization, this provides an overview of the symmetry in the Brillouin zone. The band schematic in Fig. 4b makes use of the measured band positions at Γ and the calculated Fermi level crossings of the non-CDW state, the nested band being doubly degenerate. The $\mathbf{q}_1$ zone boundary induces backfolding of both bands. For the nested band with $k_F = q_1/2$ a pseudo-Peierls gap occurs, and the lower band will exhibit a hybridization gap. Experimental observation of the bands near the $\mathbf{q}_1$ ZB is affected by (i) analogous fluctuations for $\mathbf{q}_2$ with proximity of its diagonal boundaries, and (ii) a greatly reduced CDW correlation length at RT which leads to a smearing of the backfolded features.

How can such distortion be observed at room temperature, while the CDW transition takes place at $T_1 = 145$ K? This follows from the rather one-dimensional electronic structure being susceptible to thermal fluctuations above the critical temperature T_1 which lead to short range order. X-ray diffraction measurements on $NbSe_3$ show faint diffuse intensity corresponding to the CDW vectors $\mathbf{q}_1$ and $\mathbf{q}_2$ up to room temperature [17,18]. Temperature-dependent tunneling spectroscopy measurements of the T_1 CDW energy gap [6] found a value of $2\Delta \sim 170$ meV at low temperature, and a pseudogap could be traced to a magnitude of $\sim$100 meV at 250 K before the signal was lost. In

photoemission, a pseudogap has been observed close to the Peierls metal-insulator transition in anorganic and organic 1D compounds [19,20]. However, in a 1D system a pseudogap may coexist with Luttinger liquid behavior which also removes the Fermi cutoff. Even if Peierls physics is assumed dominant, determination of the gap magnitude in the fluctuation regime is not straightforward because a pseudogap lacks a sharp edge [21]. The present data on $NbSe_3$ now demonstrate that even for $T > 2T_1$ conventional metallic band crossings are absent and the symmetry of the electronic band structure is still broken. To our knowledge, this effect has not previously been observed directly.

Quasi-one-dimensional character of the electron system is a prerequisite for the existence of fluctuations and has been checked normal to the main axis. The bands orthogonal to the sample (along width c^*) remain at constant binding energy within the experimental uncertainty. Along depth a^*, a change of the band energies on the scale of a tenth eV is observed, as expected on the basis of the DFT results. This implies a slight dispersion in the perpendicular direction, but otherwise pronounced 1D confinement.

The remnant CDW is characterized by a correlation function. An estimate for the temperature-dependent correlation length ξ can be obtained from fluctuations of the electron energy on the scale of the thermal energy [21]. The 1D correlation length for $\mathbf{q}_1$ derived as $\hbar v_F/\pi kT$ and using the DFT Fermi velocity v_F amounts to $\xi \sim 30$ Å at 300 K. Neutron scattering determines roughly similar values of 15–45 Å [17,18]. Equivalently, scattering from the superstructure has a linewidth of the order of $\xi^{-1} \sim 0.03$ Å^{-1}, which is considerable compared to the nesting vector $q_1 = 0.44$ Å^{-1}. This implies a softened Bragg scattering condition for the electron system, and the bands become broadened by the inverse correlation length. Under these conditions the symmetry-broken band structure continues to exist. The nested Fermi surface therefore is still not fully metallic at room temperature. All earlier work on temperature-dependent conductivity [5,6] accordingly reflects changes in the CDW correlation and the pseudogap which agglomerates weight at the Fermi level with increasing temperature.

In conclusion, the fluctuating Peierls system $NbSe_3$ was explored by photoemission for effects on the electronic states near the Fermi level. Band crossings at E_F needed for CDW nesting are established. In the regime well above the two critical temperatures, the zone boundaries of the broken-symmetry state are found to be still valid for the electronic states. This is not only a direct observation of consequences from structural fluctuations, but also implies that the conductivity properties of low-dimensional metallic wires are significantly modified by such fluctuating instabilities.

The authors are grateful to M. Sing for valuable technical support. This work was supported by the U.S. DOE under Grant No. DE-FG06-86ER45275 and for the ALS under Grant No. DE-AC03-76SF00098.

[1] R. E. Peierls, *Quantum Theory of Solids* (Clarendon, Oxford, 1964).
[2] J. M. Luttinger, J. Math. Phys. (N.Y.) **4**, 1154 (1963).
[3] M. Grioni and J. Voit, in *Electronic Spectroscopies Applied to Low-Dimensional Materials,* edited by H. Starnberg and H. Hughes (Kluwer, Dordrecht, 2000).
[4] J. Voit *et al.,* Science **290**, 501 (2000).
[5] N. P. Ong and P. Monceau, Phys. Rev. B **16**, 3443 (1977).
[6] H. Haifeng and Z. Dianlin, Phys. Rev. Lett. **82**, 811 (1999).
[7] A. Fournel *et al.,* Phys. Rev. Lett. **57**, 2199 (1986).
[8] See review articles by P. Monceau, G. Grüner, and J. P. Pouget, in *Physics and Chemistry of Low-Dimensional Inorganic Conductors,* edited by C. Schlenker *et al.,* NATO-ASI, Vol. 254 (Plenum, New York, 1996).
[9] R. E. Thorne, Phys. Rev. B **45**, 5804 (1992).
[10] J. A. Wilson, Phys. Rev. B **19**, 6456 (1979).
[11] J. L. Hodeau *et al.,* J. Phys. C **11**, 4117 (1978).
[12] E. Canadell *et al.,* Inorg. Chem. **29**, 1401 (1990).
[13] N. Shima, J. Phys. Soc. Jpn. **52**, 578 (1983).
[14] J. P. Perdew, K. Burke, and M. Ernzerhof, Phys. Rev. Lett. **77**, 3865 (1996).
[15] P. Blaha, K. Schwarz, and J. Luitz, WIEN97 code [improved version of P. Blaha *et al.,* Comput. Phys. Commun. **59**, 339 (1990)].
[16] J. Schäfer *et al.,* Phys. Rev. Lett. **83**, 2069 (1999).
[17] J. P. Pouget *et al.,* J. Phys. (Paris) **44**, 1729 (1983).
[18] A. H. Moudden *et al.,* Phys. Rev. Lett. **65**, 223 (1992).
[19] B. Dardel *et al.,* Phys. Rev. Lett. **67**, 3144 (1991).
[20] F. Zwick *et al.,* Phys. Rev. Lett. **81**, 2974 (1998).
[21] G. Grüner, *Density Waves in Solids* (Addison-Wesley Publishing, Reading, 1994), Chap. 5.